Supporting information for: New insights into the cooling of the oceanic lithosphere from surface-wave tomographic inferences

Franck Latallerie[1], Paula Koelemeijer[1], Andrew Walker[1], Alessia Maggi[2], Sophie Lambotte[2], Christophe Zaroli[2]

[1]Department of Earth Sciences, University of Oxford, Oxford, United Kingdom
[2]Institut Terre et Environement de Strasbourg, UMR7063, Université de Strasbourg, EOST/CNRS, 67084, Strasbourg, France

Supporting information

This supporting information file contains details on our finite-frequency SOLA tomography method, as well as Table 1, Figures S1 to S5, and references to seismic networks.

Finite-frequency surface-wave tomography using SOLA

Here, we detail the tomographic method and the resolution filtering process. Further details can be found in Latallerie et al. (2025).

Model parameterisation and setup

We measure the Rayleigh-wave phase-delays for a set of source-receiver-frequency triplets. We note d_i the datum for triplet i ($1 \leq i \leq N$). For each triplet, we compute the associated 3D finite-frequency sensitivity kernel $K_i(\boldsymbol{x})$ using the theory (and codes) derived by Zhou et al. (2004) and references therein. These sensitivity kernels take value at every location $\boldsymbol{x}$ in the 3D space $\bigoplus$ and relate the data linearly to the $\delta \ln V_{SV}$ variations $m(\boldsymbol{x})$ in the 3D space: $d_i = \iiint_{\boldsymbol{x} \in \bigoplus} K_i(\boldsymbol{x}) m(\boldsymbol{x}) d^3\boldsymbol{x}$. This is fundamentally different from previous surface-wave models such as SS2DPacific (Latallerie et al., 2022) that consist of 2D layers.

We parameterise the 3D space into a grid of 3D voxels, indexed with j ($1 \leq j \leq M$), each one with a volume V_j. In the following, we use the Einstein's summation convention, unless explicitely stated otherwise. Using this parameterisation, the forward problem becomes: $d_i = G_{ij} m_j$, where $G_{ij} = K_{ij} V_j$ (without summation), and K_{ij} is the value of the sensitivity kernel i interpolated in cell j, V_j the volume of cell j, and m_j the velocity variations $\delta \ln V_{SV}$ interpolated in cell j. When considering many data, these linear relations can be combined and written in matrix form: $\boldsymbol{d} = \boldsymbol{G}\boldsymbol{m}$.

It is important to note that the forward problem relates the data directly to the 3D $\delta \ln V_{SV}$ variations through only one linear equation. In contrast, typically employed approaches in surface-wave tomography require two steps (e.g. in the SS2DPacific model also presented), either first one that relates the raw data to 1D $\delta \ln V_{SV}$ structure with depth along a certain path, followed by another step between this 1D path-averaged $\delta \ln V_{SV}$ structure and the lateral (2D) distribution of $\delta \ln V_{SV}$ at a certain depth; or first one that relates the raw data to the lateral (2D) distribution of $\delta \ln V_{SV}$ at a certain frequency (phase or group-velocity maps), followed by another step that relates lateral variations in $\delta \ln V_{SV}$ at various frequencies to the 1D distribution of $\delta \ln V_{SV}$ versus depth at each lateral location. Neither of these approaches is set up in a truly 3D framework, such that any resolution analysis in these cases is inherently 2D or 1D (and uncertainty propagation needs to account for the two-step nature of the process).

SOLA inferences

SOLA inference is local, conducted independently for each model parameter of interest (Zaroli, 2016). Let us concentrate on estimating $\delta \ln V_{SV}$ in voxel k: $\widetilde{m}^{(k)}$. Here, we use tilde ($\widetilde{\ }$) to indicate that this is an estimate and we use the index k instead of j for reasons that will become clear later. Additionally, we use the upper-script notation to emphasize the local nature of the reasoning. We search for a model estimate that is a linear combination of the data: $\widetilde{m}^{(k)} = G^{\dagger}{}_i^{(k)} d_i$, where $\boldsymbol{G^{\dagger(k)}}$ is the vector that contains the weights of the linear combination. How should we build $\boldsymbol{G^{\dagger(k)}}$? To decide on this, we need to investigate the role it plays. Replacing d_i in the last expression using the forward relationship $d_i = G_{ij} m_j$, we obtain $\widetilde{m}^{(k)} = G^{\dagger}{}_i^{(k)} G_{ij} m_j$. This tells us that the model estimate for parameter k is an average over all true model parameters, with the averaging given by the vector $\boldsymbol{A^{(k)}}$ with components $A_j^{(k)} = G^{\dagger}{}_i^{(k)} G_{ij}$. This is the resolving kernel for model parameter k (though in practice we also take the volume of the voxels into account). The use of two letters, j or k, to identify the grid voxels becomes clear here, as j identifies the native physical model parameters $\delta \ln V_{SV}$, while k identifies a given local average.

The shape of the resolving kernel is controlled by $\boldsymbol{G}^{\dagger(\boldsymbol{k})}$. Based on this geometrical interpretation, we thus want to design $\boldsymbol{G}^{\dagger(\boldsymbol{k})}$ such that the resolving kernel is as focused as possible around the location of model parameter k. To achieve this, we design a target resolving kernel, and solve an optimisation problem based on the minimisation of the squared differences between the target kernel and the resolving kernel. Last, but not least, for a linear forward problem, we can express the estimated model uncertainty $C_{\tilde{m}_k}$ as a function of the data uncertainties C_{d_i}: $C_{\tilde{m}_k} = {G^{\dagger}}_i^{(k)^2} C_{d_i}^2$. Thus, we realise that $\boldsymbol{G}^{\dagger(\boldsymbol{k})}$ also controls the propagation of data uncertainty into model uncertainty. The higher the resolution, the stronger the propagation of uncertainty as well, leading to a resolution-uncertainty trade-off. SOLA computes $\boldsymbol{G}^{(k)}$ by optimising the balancing between the fit to the target resolution and the uncertainty propagation. Finally, from $\boldsymbol{G}^{(k)}$, we can compute the model estimate, its uncertainty, and the 3D resolving kernel (see Figure 10 in Latallerie et al. (2025)).

The process described above can be repeated for every single (or a chosen set of) model parameters, which can be visualised as a *tomographic model*. However, it is now clear that every single model parameter in this *tomographic model* is in fact a local average of the true model parameters (with some associated uncertainty and limited resolution). The advantage of SOLA is two-fold: firstly, we have direct control over the model resolution, as we push it towards some target resolution (for example one may prefer a broader, but well behaved, circular-shaped resolution over a higher, but very irregular resolution); secondly, we obtain the resolution (and uncertainty) by construction for each model parameter of interest. It is worth repeating that, since our finite-frequency framework is fundamentally 3D, the resolving kernels, obtained for every model parameter in the 3D space, are also functions of the 3D space themselves. This is a major advance compared to former implementations of SOLA with surface waves (including model SS2DPacific), and it allows us to discuss 3D resolution effects in surface-wave tomography, especially with depth.

Tomographic filtering of predictions

Imagine we have predictions for the $\delta \ln V_{SV}$ structure (m_j^{pred}) for a set of voxels j. The physical meaning of the predictions and the tomographic model are very different. While the prediction provides physical parameters at absolute locations in space, the tomographic model consists of a set of local averages of these parameters. Therefore, any meaningful comparison between the tomographic model and the predictions should start by applying the local averaging (through the resolving kernels) to the predictions; a process commonly known as 'tomographic filtering'. If the resolution for the tomographic model is available (a rare commodity though, especially in 3D for surface-waves), the process is relatively straightforward: compute $\widetilde{m^{\text{pred}}}^{(k)} = {G^{\dagger}}_i^{(k)} G_{ij} m_j^{\text{pred}}$. $\widetilde{m^{\text{pred}}}^{(k)}$ is the filtered prediction, which is now directly comparable to the tomographic model.

In this study, we show that tomographic filtering has a large impact on predictions of the thermal structure of the oceanic lithosphere based on the plate cooling (PC) and half-space cooling (HSC) models. We use the modified plate cooling (PC) model from Richards et al. (2018), denoted as $T^{\text{PC}}(t, z)$, where z is the depth and t is the age of the lithosphere. To link geographic locations to age $t(\theta, \phi)$, we use the age model of Seton et al. (2020), where θ and ϕ denote latitude and longitude. We can therefore compute predictions at every location in the 3D tomographic grid: ${m^{PC}}_j = T^{\text{PC}}(t(\theta_j, \phi_j), z_j)$, where θ_j, ϕ_j, and z_j are the latitude, longitude and depth of the centre of voxel j. Subsequently, we compute the filtered predictions as $\widetilde{m^{\text{PC}}}^{(k)} = {G^{\dagger}}_i^{(k)} G_{ij} m_j^{\text{PC}}$, which we can then compare to the model estimates from our 3D surface-wave tomography. We follow the same process for the HSC model, except that the

temperature field is given by the equations and constants from Stein and Stein (1992): $T^{\mathrm{HSC}}(t,z) = T_m \mathrm{erf}(z/\sqrt{4\kappa t})$, where $T_m = 1350°C$ is the mantle potential temperature, $\kappa = k/(\rho_m C_p)$ is the thermal diffusivity, with $k = 3.138$ J s^{-1} m^{-1} K^{-1} the thermal conductivity and $C_p = 1171$ J K^{-1} kg^{-1} the specific heat capacity, and erf(.) the error function.

Using the above filtering approach, we demonstrate that the differences between the non-filtered and filtered predictions (namely between ${m^{\mathrm{PC}}}_j$ and $\widetilde{m^{\mathrm{PC}}}^{(k)}$, as well as between ${m^{\mathrm{HSC}}}_j$ and $\widetilde{m^{\mathrm{HSC}}}^{(k)}$) are large and cannot be ignored. Resolution does not only add random noise in the model, it introduces artificial structures that can be extremely misleading. This is particularly true with depth, where the complex sensitivity of surface waves with depth leads to a poorly behaved 3D resolution.

Note on the parameterisation

The parameterisation should be chosen as small as possible. Any discrepancy between the continuous sensitivity kernels and their discretised counterparts represents a theoretical error that should be added to the global uncertainty. Therefore, the smaller the voxels, the smaller this uncertainty contribution. Visual screening of the sensitivity kernels show that they retain their main properties. This has been investigated more in detail in Latallerie et al. (2025).

Additonally, the parameterisation should be small enough to honor the conceptual shape of the continuous target kernels. In this study, the parameterisation is relatively coarse compared to the size of the target kernels, which, additionally, are chosen relatively small. However, as long as we are satisfied with the discretised versions of the target kernels themselves, there is no drawback. Here, the projected target kernels resemble 'Dirac delta'-kernels, consequently the SOLA method attempts to construct resolution kernels that are as small as possible, given the limitations imposed by the uncertainty and chosen tradeoff parameter.

Tables and figures

Table 1. Details of tomography models shown in Figure 5 and Figure S1

Name	Forward	Inverse	Parameters	Parameterisation	Data	Domain
SS3DPacific	Born FF	SOLA 3D	Vsv	Local	R fund. phase	Uppermost-mantle
SS2DPacific	Ray	Data-misfit + SOLA 2D	Vsv	Local	R multi. phase	Upper-mantle
FFSW1	Born FF	Data-misfit	Vsv, Vsh	Local	R/G fund. phase	Upper-mantle
REVEAL	Adjoint	Data-misfit	Vsv, Vsh, Vp	Local	Full-waveform	Whole-mantle
GLAD-M35	Adjoint	Data-misfit	Vsv, Vsh, Vp, eta	Local	Full-waveform	Whole-mantle
SEMUCB-WM1	SEM-NACT	Data-misfit	Vs, Vsh/Vsv	Local	Full-waveform	Whole-mantle
SGLOBE-RANI	Ray	Data-misfit	Vs, $\frac{Vsh^2-Vsv^2}{2Vs^2}$, ρ	Global	R/G multi. phase/group, TT	Whole-mantle
S362ANI	Ray	Data-misfit	Vs, Vsh-Vsv, Vph-Vpv	Global	R/G fund. phase, body waveform, TT	Whole-mantle

FF: Finite-frequency, R: Rayleigh, G: Love, fund.: fundamental, multi.: multimode, TT: Body-wave traveltimes, ρ: density.

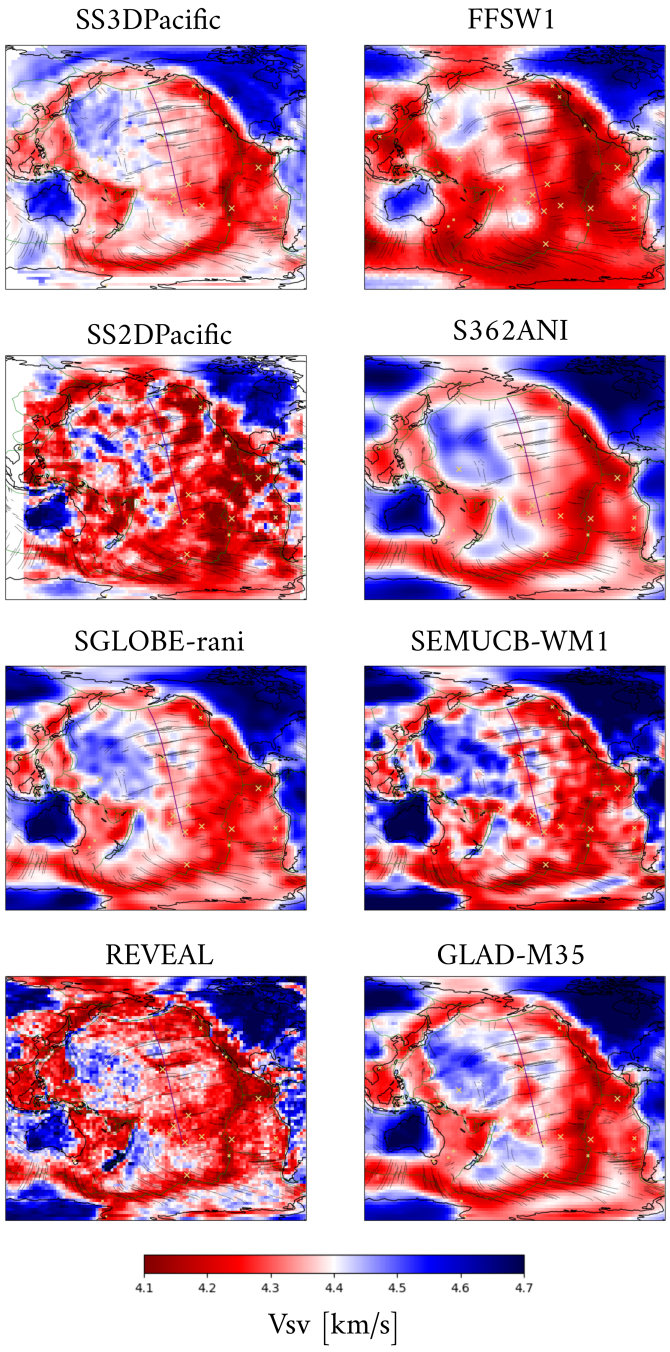

Figure S1. Comparison of the absolute Vsv structure of SS3DPacific compared to a selection of tomography models at 112 km depth. We include SS2DPacific (Latallerie et al., 2022), SGLOBE-rani (Chang et al., 2015), REVEAL:(Thrastarson et al., 2024), FFSW1 (Zhou et al., 2006), S362ANI (Kustowski et al., 2008), SEMUCB-WM1 (French & Romanowicz, 2014), and GLAD-M35 (Cui et al., 2024).

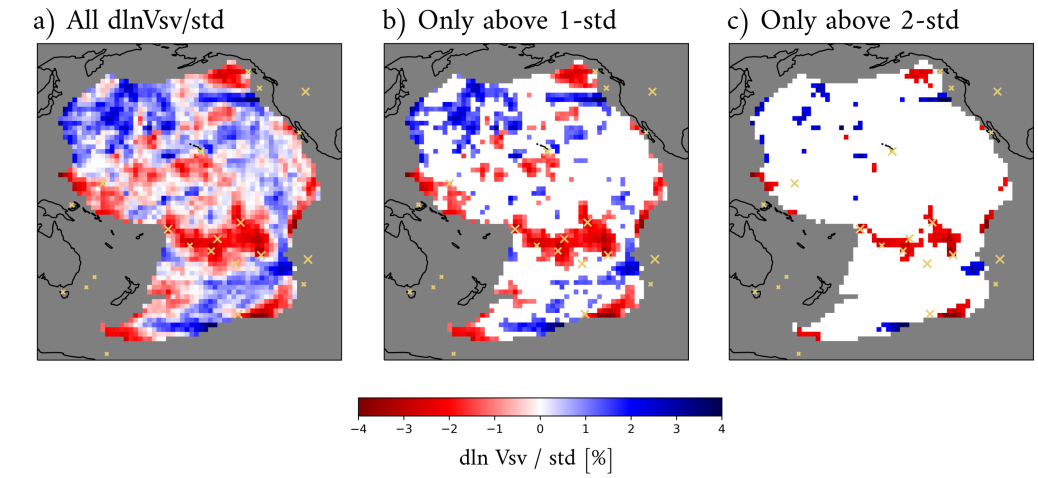

Figure S2. Significant lateral features in SS3DPacific, obtained by removing the age-dependence trend (of SS3DPacific itself) and normalising by the model uncertainty (std). We include a) all features, or mask values below b) the 1-σ or c) the 2-σ level. Yellow crosses indicate hotspot locations, see the caption of Figure 1 in the main text.

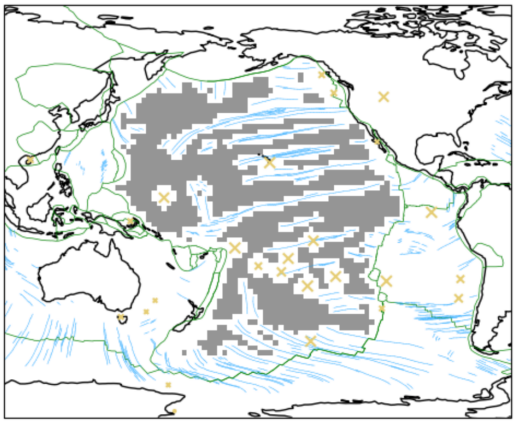

Figure S3. Mask used to calculate the trends of the average velocity with age. Grey cells indicate regions that are included, while regions near hotspots (yellow crosses), fracture zones (black lines), and plate boundaries (green lines) are excluded. See the caption of Figure 1 in the main text for more details.

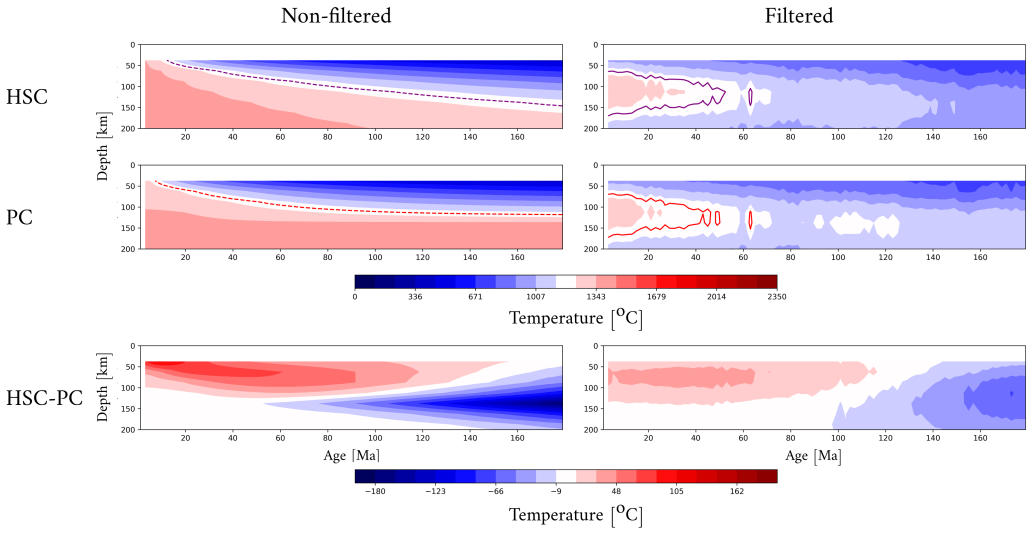

Figure S4. Thermal structure according to models HSC (first row) and PC (second row), as well as their differences (last row). The left column shows the original, non-filtered thermal structure and the second column shows the filtered version using the SS3DPacific tomographic filter. Purple and red dashed lines represent the 1175°C isotherm of the HSC and PC models, respectively, while their solid counterparts represent the same isotherm, but for the filtered versions of these models.

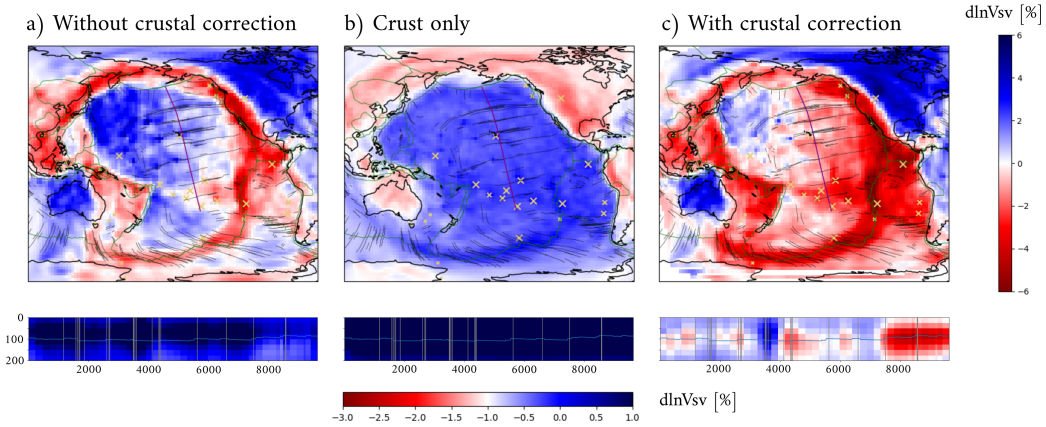

Figure S5. Assessment of influence of crustal structure on the model solution, showing results at 112 km depth for SOLA inference of a) data without crustal corrections applied, b) only predictions for crustal structure, and c) data with crustal corrections (i.e. SS3DPacific). We use a different colorscale for the cross-sections to better represent the range of velocities shown.

Citations for seismic networks used in this study

We list here the network codes (in bold) for stations analysed in this study followed by the full citation as per the FDSN website, where available.

- **IP**: Anya Reading and Nick Rawlinson (2011); Ritter et al. (2014); Douglas Wiens and Maria Beatrice Magnani (2018); Sarah Mader et al. (2022)
- **6E** James Conder (2013); John Louie (2018); Pieter-Ewald Share and Frank Vernon (2019); Elnaz Seylabi et al. (2021); Dahm et al. (2023); Susan Bilek (2024)
- **7A** Ryberg and Haberland (2008); Ramon Carbonell (2012); Maureen Long and Paul Wiita (2013); Nicholas Schmerr (2017); Christopher W Johnson et al. (2018); Yuan et al. (2019); Marcelo Rocha (2021); Neil Harbison and Craig O'Neill (2024)
- **7C** Vergne et al. (2014); Rufus Catchings (2014); Derek Schutt and Rick Aster (2015); Costanzo et al. (2022)
- **7D** Brian Kennett (1997); Wes Thelen and Paul Bodin (2009); IRIS OBSIP (2011); Wenyuan Fan et al. (2018); Calum Chamberlain (2022)
- **AE** Arizona Geological Survey (2007)
- **AI** Istituto Nazionale di Oceanografia e di Geofisica Sperimentale (1992)
- **AK** Alaska Earthquake Center, Univ. of Alaska Fairbanks (1987)
- **AR** No DOI
- **AT** NOAA National Oceanic and Atmospheric Administration (USA) (1967)
- **AU** Geoscience Australia (2021)
- **AV** Alaska Volcano Observatory-USGS (1988)
- **AZ** Frank Vernon (1982)
- **BK** Northern California Earthquake Data Center (2014)
- **C** No DOI
- **C1** Universidad de Chile (2012)
- **CB** Institute of Geophysics China Earthquake Administration (IGPCEA) (2000)
- **CC** Cascades Volcano Observatory/USGS (2001)
- **CI** California Institute of Technology and United States Geological Survey Pasadena (1926)
- **CM** Servicio Geológico Colombiano (1993)
- **CN** Natural Resources Canada (1975)
- **CU** Albuquerque Seismological Laboratory (ASL)/USGS (2006)
- **DK** GEUS Geological Survey of Denmark and Greenland (1976)
- **G** Institut de physique du globe de Paris (IPGP) and École et Observatoire des Sciences de la Terre de Strasbourg (EOST) (1982)
- **GG** IRIS HQ (DC) (2012)
- **GS** Albuquerque Seismological Laboratory (ASL)/USGS (1980)
- **GT** Albuquerque Seismological Laboratory (ASL)/USGS (1993)
- **IC** Albuquerque Seismological Laboratory (ASL)/USGS (1992)
- **II** Scripps Institution of Oceanography (1986)
- **IM** Various Institutions (1965)
- **IU** Albuquerque Seismological Laboratory/USGS (1988)
- **JP** No DOI
- **KS** No DOI
- **LB** No DOI
- **LD** Lamont Doherty Earth Observatory (LDEO), Columbia University (1970)
- **MI** USGS Alaska Anchorage (2000)
- **MM** Department of Meteorology and Hydrology - National Earthquake Data Center (2016)

- **MX** Servicio Sismológico Nacional, Instituto de Geofísica, Universidad Nacional Autónoma de México, México (2017)
- **MY** No DOI
- **N4** Albuquerque Seismological Laboratory/USGS (2013)
- **NA** KNMI (2006)
- **NE** Albuquerque Seismological Laboratory (ASL)/USGS (1994)
- **NM** No DOI
- **NN** University of Nevada, Reno (1971)
- **NR** Utrecht University (UU Netherlands) (1983)
- **NU** Instituto Nicaraguense de Estudios Territoriales (INETER) (1975)
- **OO** NSF Ocean Observatories Initiative (2013)
- **PB** No DOI
- **PE** Penn State University (2004)
- **PN** No DOI
- **PR** University of Puerto Rico (1986)
- **PS** No DOI
- **PY** Frank Vernon (2014)
- **RM** Regional Integrated Multi-Hazard Early Warning System (RIMES Thailand) (2008)
- **RV** Alberta Geological Survey / Alberta Energy Regulator (2013)
- **S1** Michelle Salmon et al. (2011)
- **SC** New Mexico Tech (1999)
- **SV** No DOI
- **TA** IRIS Transportable Array (2003)
- **TM** No DOI
- **TW** Institute of Earth Sciences, Academia Sinica, Taiwan (1996)
- **TX** Bureau of Economic Geology, The University of Texas at Austin (2016)
- **UO** University of Oregon (1990)
- **US** Albuquerque Seismological Laboratory (ASL)/USGS (1990)
- **UW** University of Washington (1963)
- **WI** Institut De Physique Du Globe De Paris (IPGP) (2008)
- **XF** Frank Vernon and Jon Fletcher (1987); Steve Day and Frank Vernon (1994); Sridhar Anandakrishnan (1995); Frank Vernon and Ken Dueker (2000); John Nabelek (2002); Steve Grand and Jim Ni (2006); Chris Larsen and Michael West (2009); Douglas Wiens (2012); Meredith Nettles (2014); S. De Angelis and A. Diaz-Moreno (2017); Tiberi et al. (2020); Haberland et al. (2021); Anne Meltzer et al. (2021); Pilz et al. (2023); Paul et al. (2024)
- **XZ** Rick Aster and Philip Kyle (1999); Anthony Qamar (2001); Sylvie Leroy (2003); Roger Hansen and Gary Pavlis (2005); Chris Hayward (2014); Christian Poppeliers (2015); Frank Kruger et al. (2016); Silvio De Angelis (2018); Andy Nyblade (2019); SOCQUET et al. (2020)
- **Y6** Ian Joughin et al. (2006); Keir et al. (2016); Jamie Farrell et al. (2018); John Louie and Ronald Breitmeyer (2019); Tilmann et al. (2021); Weisen Shen (2023)
- **YP** Steve Grand and Jim Ni (2009); Zhao et al. (2016); Cornou et al. (2014); Gordon Hamilton (2016); Doubre et al. (2021); Amanda Bustin (2019)
- **Z7** Dan Klinglesmith (2008); Robert White (2010); Paul Bedrosian et al. (2017); Vergne and RESIF (2021); Tulane University et al. (2019); Dietrich Lange and Marcos Moreno (2023); Noah Finnegan and Susan Schwartz (2023)

References

Alaska Earthquake Center, Univ. of Alaska Fairbanks. (1987). *Alaska geophysical network.* International Federation of Digital Seismograph Networks. Retrieved from https://www.fdsn.org/networks/detail/AK/ doi: 10.7914/SN/AK

Alaska Volcano Observatory-USGS. (1988). *Alaska volcano observatory.* International Federation of Digital Seismograph Networks. Retrieved from https://www.fdsn.org/networks/detail/AV/ doi: 10.7914/SN/AV

Alberta Geological Survey / Alberta Energy Regulator. (2013). *Regional alberta observatory for earthquake studies network.* International Federation of Digital Seismograph Networks. Retrieved from https://www.fdsn.org/networks/detail/RV/ doi: 10.7914/SN/RV

Albuquerque Seismological Laboratory (ASL)/USGS. (1980). *Us geological survey networks.* International Federation of Digital Seismograph Networks. Retrieved from https://www.fdsn.org/networks/detail/GS/ doi: 10.7914/SN/GS

Albuquerque Seismological Laboratory (ASL)/USGS. (1990). *United states national seismic network.* International Federation of Digital Seismograph Networks. Retrieved from https://www.fdsn.org/networks/detail/US/ doi: 10.7914/SN/US

Albuquerque Seismological Laboratory (ASL)/USGS. (1992). *New china digital seismograph network.* International Federation of Digital Seismograph Networks. Retrieved from https://www.fdsn.org/networks/detail/IC/ doi: 10.7914/SN/IC

Albuquerque Seismological Laboratory (ASL)/USGS. (1993). *Global telemetered seismograph network (usaf/usgs).* International Federation of Digital Seismograph Networks. Retrieved from https://www.fdsn.org/networks/detail/GT/ doi: 10.7914/SN/GT

Albuquerque Seismological Laboratory (ASL)/USGS. (1994). *New england seismic network.* International Federation of Digital Seismograph Networks. Retrieved from https://www.fdsn.org/networks/detail/NE/ doi: 10.7914/SN/NE

Albuquerque Seismological Laboratory (ASL)/USGS. (2006). *Caribbean network.* International Federation of Digital Seismograph Networks. Retrieved from https://www.fdsn.org/networks/detail/CU/ doi: 10.7914/SN/CU

Albuquerque Seismological Laboratory/USGS. (1988). *Global seismograph network (gsn - iris/usgs).* International Federation of Digital Seismograph Networks. Retrieved from https://www.fdsn.org/networks/detail/IU/ doi: 10.7914/SN/IU

Albuquerque Seismological Laboratory/USGS. (2013). *Central and eastern us network.* International Federation of Digital Seismograph Networks. Retrieved from https://www.fdsn.org/networks/detail/N4/ doi: 10.7914/SN/N4

Amanda Bustin. (2019). *Ubcism.* International Federation of Digital Seismograph Networks. Retrieved from https://www.fdsn.org/networks/detail/YP_2019/ doi: 10.7914/SN/YP_2019

Andy Nyblade. (2019). *Shale hills critical zone observatory mini-array experiment.* International Federation of Digital Seismograph Networks. Retrieved from https://www.fdsn.org/networks/detail/XZ_2019/ doi: 10.7914/SN/XZ_2019

Anne Meltzer, Susan Beck, & Joshua Stachnik. (2021). *High resolution imaging of the pedernales earthquake rupture zone - broadbands.* International Federation of Digital Seismograph Networks. Retrieved from https://www.fdsn.org/networks/detail/XF_2021/ doi: 10.7914/SN/XF_2021

Anthony Qamar. (2001). *Spokane wa earthquake swarm.* International Federation of Digital Seismograph Networks. Retrieved from https://www.fdsn.org/networks/detail/XZ_2001/ doi: 10.7914/SN/XZ_2001

Anya Reading, & Nick Rawlinson. (2011). *Bass strait.* International Federation of Digital Seismograph Networks. Retrieved from https://www.fdsn.org/

networks/detail/1P_2011/ doi: 10.7914/SN/1P_2011

Arizona Geological Survey. (2007). *Arizona broadband seismic network.* International Federation of Digital Seismograph Networks. Retrieved from https://www.fdsn.org/networks/detail/AE/ doi: 10.7914/SN/AE

Brian Kennett. (1997). *Kimba97.* International Federation of Digital Seismograph Networks. Retrieved from https://www.fdsn.org/networks/detail/7D_1997/ doi: 10.7914/SN/7D_1997

Bureau of Economic Geology, The University of Texas at Austin. (2016). *Texas seismological network.* International Federation of Digital Seismograph Networks. Retrieved from https://www.fdsn.org/networks/detail/TX/ doi: 10.7914/SN/TX

California Institute of Technology and United States Geological Survey Pasadena. (1926). *Southern california seismic network.* International Federation of Digital Seismograph Networks. Retrieved from https://www.fdsn.org/networks/detail/CI/ doi: 10.7914/SN/CI

Calum Chamberlain. (2022). *Puysegur tremor and nucleation geophysical observatory.* International Federation of Digital Seismograph Networks. Retrieved from https://www.fdsn.org/networks/detail/7D_2022/ doi: 10.7914/SN/7D_2022

Cascades Volcano Observatory/USGS. (2001). *Cascade chain volcano monitoring.* International Federation of Digital Seismograph Networks. Retrieved from https://www.fdsn.org/networks/detail/CC/ doi: 10.7914/SN/CC

Chang, S.-J., Ferreira, A. M. G., Ritsema, J., van Heijst, H. J., & Woodhouse, J. H. (2015, June). Joint inversion for global isotropic and radially anisotropic mantle structure including crustal thickness perturbations: RADIALLY ANISOTROPIC MANTLE STRUCTURE. *Journal of Geophysical Research: Solid Earth*, *120*(6), 4278–4300. Retrieved 2023-02-06, from http://doi.wiley.com/10.1002/2014JB011824 doi: 10.1002/2014JB011824

Chris Hayward. (2014). *Idaho teton dam.* International Federation of Digital Seismograph Networks. Retrieved from https://www.fdsn.org/networks/detail/XZ_2014/ doi: 10.7914/SN/XZ_2014

Chris Larsen, & Michael West. (2009). *Collaborative research: Relating glacier-generated seismicity to ice motion, basal processes and iceberg calving.* International Federation of Digital Seismograph Networks. Retrieved from https://www.fdsn.org/networks/detail/XF_2009/ doi: 10.7914/SN/XF_2009

Christian Poppeliers. (2015). *Measuring ambient noise of ocean breakers.* International Federation of Digital Seismograph Networks. Retrieved from https://www.fdsn.org/networks/detail/XZ_2015/ doi: 10.7914/SN/XZ_2015

Christopher W Johnson, Frank Vernon, Yehuda Ben-Zion, & Norimitsu Nakata. (2018). *Sage brush flats seismic experiment on interaction of wind with ground motion.* International Federation of Digital Seismograph Networks. Retrieved from https://www.fdsn.org/networks/detail/7A_2018/ doi: 10.7914/SN/7A_2018

Cornou, C., Bard, P.-Y., & RESIF. (2014). *Seismic network yp:french part of the argostoli (greece) aftershock experiment (resif-sismob).* RESIF - Réseau Sismologique et géodésique Français. Retrieved from https://seismology.resif.fr/networks/\#/YP__2014 doi: 10.15778/RESIF.YP2014

Costanzo, A., Falcone, S., La Piana, C., Caserta, A., Doumaz, F., Buongiorno, M. F., ... Speciale, S. (2022, April). *Urban Seismic Network (RUSN-CALINGV) - Real time Urban Seismic Network managed by CALabrian headquarters of INGV for monitoring urban areas, critical infrastructures and cultural heritage sites.* Istituto Nazionale di Geofisica e Vulcanologia (INGV). Retrieved from https://eida.ingv.it/en/network/7C_2021 (Artwork Size: 1 GB per day Pages: 1 GB per day) doi: 10.13127/SD/O5NRHMP9N7

Cui, C., Lei, W., Liu, Q., Peter, D., Bozdağ, E., Tromp, J., ... Pugmire, D. (2024,

August). GLAD-M35: a joint P and S global tomographic model with uncertainty quantification. *Geophysical Journal International*, *239*(1), 478–502. Retrieved 2025-07-18, from https://academic.oup.com/gji/article/239/1/478/7727823 (Publisher: Oxford University Press (OUP)) doi: 10.1093/gji/ggae270

Dahm, T., Isken, M. P., Milkereit, C., Mikulla, S., Yuan, X., Sens-Schönfelder, C., ... Busch, S. (2023). *Eifel large-n seismic network (elsn).* GFZ Data Services. Retrieved from https://geofon.gfz-potsdam.de/doi/network/6E/2022 doi: 10.14470/1R080930

Dan Klinglesmith. (2008). *Mroi vibration studies.* International Federation of Digital Seismograph Networks. Retrieved from https://www.fdsn.org/networks/detail/Z7_2008/ doi: 10.7914/SN/Z7_2008

Department of Meteorology and Hydrology - National Earthquake Data Center. (2016). *Myanmar national seismic network.* International Federation of Digital Seismograph Networks. Retrieved from https://www.fdsn.org/networks/detail/MM/ doi: 10.7914/SN/MM

Derek Schutt, & Rick Aster. (2015). *The mackenzie mountains transect: Active deformation from margin to craton.* International Federation of Digital Seismograph Networks. Retrieved from https://www.fdsn.org/networks/detail/7C_2015/ doi: 10.7914/SN/7C_2015

Dietrich Lange, & Marcos Moreno. (2023). *So297-land: Onshore extension of the 2023 rv so297 eperiment between copiapó and taltal, chile.* International Federation of Digital Seismograph Networks. Retrieved from https://www.fdsn.org/networks/detail/Z7_2023/ doi: 10.7914/KHGA-FW51

Doubre, C., Leroy, S., Keir, D., Pagli, C., & RESIF. (2021). *Study of the structure of the lithosphere from the continental plateau of western ethiopia to the active afar rift (resif-sismob).* RESIF - Réseau Sismologique et géodésique Français. Retrieved from https://seismology.resif.fr/networks/\#/YP__2017 doi: 10.15778/RESIF.YP2017

Douglas Wiens. (2012). *Mantle serpentinization and water cycling through the mariana trench and forearc.* International Federation of Digital Seismograph Networks. Retrieved from https://www.fdsn.org/networks/detail/XF_2012/ doi: 10.7914/SN/XF_2012

Douglas Wiens, & Maria Beatrice Magnani. (2018). *Solid earth response of the patagonia andes to post-little ice age glacial retreat.* International Federation of Digital Seismograph Networks. Retrieved from https://www.fdsn.org/networks/detail/1P_2018/ doi: 10.7914/SN/1P_2018

Elnaz Seylabi, Scott Tyler, Rachel Hatch, & Seth Saltiel. (2021). *Sub-surface imaging of the west reno basin.* International Federation of Digital Seismograph Networks. Retrieved from https://www.fdsn.org/networks/detail/6E_2021/ doi: 10.7914/SN/6E_2021

Frank Kruger, Andreas Rietbrock, Catherine Rychert, Nicholas Harmon, & Jenny Collier. (2016). *Volatile recycling at the lesser antilles arc: Processes and consequences.* International Federation of Digital Seismograph Networks. Retrieved from https://www.fdsn.org/networks/detail/XZ_2016/ doi: 10.7914/SN/XZ_2016

Frank Vernon. (1982). *Anza regional network.* International Federation of Digital Seismograph Networks. Retrieved from https://www.fdsn.org/networks/detail/AZ/ doi: 10.7914/SN/AZ

Frank Vernon. (2014). *Piñon flats observatory array.* International Federation of Digital Seismograph Networks. Retrieved from https://www.fdsn.org/networks/detail/PY/ doi: 10.7914/SN/PY

Frank Vernon, & Jon Fletcher. (1987). *Anza borehole experiment.* International Federation of Digital Seismograph Networks. Retrieved from https://www.fdsn.org/networks/detail/XF_1987/ doi: 10.7914/SN/XF_1987

Frank Vernon, & Ken Dueker. (2000). *Laramie telemetered broad-band array.* International Federation of Digital Seismograph Networks. Retrieved from https://www.fdsn.org/networks/detail/XF_2000/ doi: 10.7914/SN/XF_2000

French, S. W., & Romanowicz, B. A. (2014, December). Whole-mantle radially anisotropic shear velocity structure from spectral-element waveform tomography. *Geophysical Journal International*, *199*(3), 1303–1327. Retrieved 2022-10-09, from http://academic.oup.com/gji/article/199/3/1303/612270/Wholemantle-radially-anisotropic-shear-velocity doi: 10.1093/gji/ggu334

Geoscience Australia. (2021). *Australian national seismograph network data collection.* Commonwealth of Australia (Geoscience Australia). Retrieved from http://pid.geoscience.gov.au/dataset/ga/144675 doi: 10.26186/144675

GEUS Geological Survey of Denmark and Greenland. (1976). *Danish seismological network.* International Federation of Digital Seismograph Networks. Retrieved from https://www.fdsn.org/networks/detail/DK/ doi: 10.7914/NW3X-DF02

Gordon Hamilton. (2016). *Flow and fracture dynamics in an ice shelf lateral margin: Observations and modeling of the mcmurdo shear zone.* International Federation of Digital Seismograph Networks. Retrieved from https://www.fdsn.org/networks/detail/YP_2016/ doi: 10.7914/SN/YP_2016

Haberland, C., Ryberg, T., & Kirsch, M. (2021). *The geyer seismic network.* GFZ Data Services. Retrieved from https://geofon.gfz-potsdam.de/doi/network/XF/2020 doi: 10.14470/KS7575632014

Ian Joughin, Sarah Das, & Mark Behn. (2006). *Behavior of supraglacial lakes and their role in outlet glacier dynamics and mass balance of the greenland ice sheet.* International Federation of Digital Seismograph Networks. Retrieved from https://www.fdsn.org/networks/detail/Y6_2006/ doi: 10.7914/SN/Y6_2006

Institut De Physique Du Globe De Paris (IPGP). (2008). *Gnss, seismic broadband and strong motion permanent networks in west indies.* Institut de physique du globe de Paris (IPGP), Université de Paris. Retrieved from http://volobsis.ipgp.fr/networks/detail/WI/ doi: 10.18715/ANTILLES.WI

Institut de physique du globe de Paris (IPGP), & École et Observatoire des Sciences de la Terre de Strasbourg (EOST). (1982). *Geoscope, french global network of broad band seismic stations.* Institut de physique du globe de Paris (IPGP), Université de Paris. Retrieved from http://geoscope.ipgp.fr/networks/detail/G/ doi: 10.18715/GEOSCOPE.G

Institute of Earth Sciences, Academia Sinica, Taiwan. (1996). *Broadband array in taiwan for seismology.* International Federation of Digital Seismograph Networks. Retrieved from https://www.fdsn.org/networks/detail/TW/ doi: 10.7914/SN/TW

Institute of Geophysics China Earthquake Administration (IGPCEA). (2000). *China national seismic network, data management centre of china national seismic network at institute of geophysics, cea.* International Federation of Digital Seismograph Networks. Retrieved from https://www.fdsn.org/networks/detail/CB/ doi: 10.7914/SN/CB

Instituto Nicaraguense de Estudios Territoriales (INETER). (1975). *Nicaraguan seismic network.* International Federation of Digital Seismograph Networks. Retrieved from https://www.fdsn.org/networks/detail/NU/ doi: 10.7914/SN/NU

IRIS HQ (DC). (2012). *Greenland ice sheet monitoring network.* International Federation of Digital Seismograph Networks. Retrieved from https://www.fdsn.org/networks/detail/GG/ doi: 10.7914/SN/GG

IRIS OBSIP. (2011). *Cascadia initiative community experiment - obs component.* International Federation of Digital Seismograph Networks. Retrieved from https://www.fdsn.org/networks/detail/7D_2011/ doi: 10.7914/SN/7D_2011

IRIS Transportable Array. (2003). *Usarray transportable array.* International Federation of Digital Seismograph Networks. Retrieved from https://www.fdsn.org/networks/detail/TA/ doi: 10.7914/SN/TA

Istituto Nazionale di Oceanografia e di Geofisica Sperimentale. (1992). *Antarctic seismographic argentinean italian network - asain.* International Federation of Digital Seismograph Networks. Retrieved from https://www.fdsn.org/networks/detail/AI/ doi: 10.7914/SN/AI

James Conder. (2013). *Wabash valley seismic zone.* International Federation of Digital Seismograph Networks. Retrieved from https://www.fdsn.org/networks/detail/6E_2013/ doi: 10.7914/SN/6E_2013

Jamie Farrell, Keith Koper, & Robert Sohn. (2018). *Yellowstone lake microseism 2018.* International Federation of Digital Seismograph Networks. Retrieved from https://www.fdsn.org/networks/detail/Y6_2018/ doi: 10.7914/SN/Y6_2018

John Louie. (2018). *Surface-wave characterization of the shoal nuclear blast cavity and rubble chimney.* International Federation of Digital Seismograph Networks. Retrieved from https://www.fdsn.org/networks-detail/6E_2018/ doi: 10.7914/SN/6E_2018

John Louie, & Ronald Breitmeyer. (2019). *Community, arts, and environmental setting of fly geyser, nevada.* International Federation of Digital Seismograph Networks. Retrieved from https://www.fdsn.org/networks/detail/Y6_2019/ doi: 10.7914/SN/Y6_2019

John Nabelek. (2002). *Collaborative research: Lithospheric scale dynamics of active mountain building along the himalayan-tibetan collision zone.* International Federation of Digital Seismograph Networks. Retrieved from https://www.fdsn.org/networks/detail/XF_2002/ doi: 10.7914/SN/XF_2002

Keir, Kendall, & Ayele. (2016). *Rift valley volcanism past present and future.* International Federation of Digital Seismograph Networks. Retrieved from https://www.fdsn.org/networks/detail/Y6_2016/ doi: 10.7914/SN/Y6_2016

KNMI. (2006). *Caribbean netherlands seismic network.* Royal Netherlands Meteorological Institute (KNMI). Retrieved from http://rdsa.knmi.nl/network/NA/ doi: 10.21944/DFFA7A3F-7E3A-3B33-A436-516A01B6AF3F

Kustowski, B., Ekström, G., & Dziewoński, A. M. (2008, June). Anisotropic shear-wave velocity structure of the Earth's mantle: A global model. *Journal of Geophysical Research*, *113*(B6), B06306. Retrieved 2022-10-03, from http://doi.wiley.com/10.1029/2007JB005169 doi: 10.1029/2007JB005169

Lamont Doherty Earth Observatory (LDEO), Columbia University. (1970). *Lamont-doherty cooperative seismographic network.* International Federation of Digital Seismograph Networks. Retrieved from https://www.fdsn.org/networks/detail/LD/ doi: 10.7914/SN/LD

Latallerie, F., Zaroli, C., Lambotte, S., & Maggi, A. (2022, April). Analysis of tomographic models using resolution and uncertainties: a surface wave example from the Pacific. *Geophysical Journal International*, *230*(2), 893–907. Retrieved 2022-04-20, from https://academic.oup.com/gji/article/230/2/893/6544670 doi: 10.1093/gji/ggac095

Latallerie, F., Zaroli, C., Lambotte, S., Maggi, A., Walker, A., & Koelemeijer, P. (2025, August). Towards surface wave tomography with 3D resolution and uncertainty: Resolution-uncertainty in 3D surface-wave tomography. *Seismica*, *4*(2). Retrieved 2025-09-02, from https://seismica.library.mcgill.ca/article/view/1407 doi: 10.26443/seismica.v4i2.1407

Marcelo Rocha. (2021). *Carajás mineral province seismic network.* International Federation of Digital Seismograph Networks. Retrieved from https://www.fdsn.org/networks/detail/7A_2021/ doi: 10.7914/SN/7A_2021

Maureen Long, & Paul Wiita. (2013). *Mid-atlantic geophysical integrative collaboration.* International Federation of Digital Seismograph Networks. Retrieved from https://www.fdsn.org/networks/detail/7A_2013/ doi: 10.7914/SN/7A_2013

Meredith Nettles. (2014). *Understanding precambrian to present assembly of greenland.* International Federation of Digital Seismograph Networks. Retrieved from https://www.fdsn.org/networks/detail/XF_2014/ doi: 10.7914/SN/XF_2014

Michelle Salmon, Natalie Balfour, Malcolm Sambridge, Sima Mousavi, & Robert Pickle. (2011). *Australian seismometers in schools.* AusPass. Retrieved from https://www.fdsn.org/networks/detail/S1/ doi: 10.7914/SN/S1

Natural Resources Canada. (1975). *Canadian national seismograph network.* Natural Resources Canada. Retrieved from https://www.fdsn.org/networks/detail/CN/ doi: 10.7914/SN/CN

Neil Harbison, & Craig O'Neill. (2024). *Georgetown seismic traverse, north queensland.* International Federation of Digital Seismograph Networks. Retrieved from https://www.fdsn.org/networks/detail/7A_2024/ doi: 10.7914/3V05-SW22

New Mexico Tech. (1999). *New mexico tech seismic network.* International Federation of Digital Seismograph Networks. Retrieved from https://www.fdsn.org/networks/detail/SC/ doi: 10.7914/0ABK-1345

Nicholas Schmerr. (2017). *Geodes san francisco volcanic field active seismic experiment 2017.* International Federation of Digital Seismograph Networks. Retrieved from https://www.fdsn.org/networks/detail/7A_2017/ doi: 10.7914/TYZX-JN40

NOAA National Oceanic and Atmospheric Administration (USA). (1967). *National tsunami warning center alaska seismic network.* International Federation of Digital Seismograph Networks. Retrieved from https://www.fdsn.org/networks/detail/AT/ doi: 10.7914/SN/AT

Noah Finnegan, & Susan Schwartz. (2023). *Nodal seismometer deployment at oak ridge earthflow near san jose, ca.* International Federation of Digital Seismograph Networks. Retrieved from https://www.fdsn.org/networks/detail/Z7_2023/ doi: 10.7914/PNFW-J315

Northern California Earthquake Data Center. (2014). *Berkeley digital seismic network (bdsn).* Northern California Earthquake Data Center. Retrieved from https://ncedc.org/bk_doi_metadata.html doi: 10.7932/BDSN

NSF Ocean Observatories Initiative. (2013). *Ocean observatories initiative.* International Federation of Digital Seismograph Networks. Retrieved from https://www.fdsn.org/networks/detail/OO/ doi: 10.7914/SN/OO

Paul, A., Mordret, A., Aubert, C., Chevrot, S., Sylvander, M., Pauchet, H., & RESIF. (2024). *Maciv-profiles temporary experiment of seismic imaging of the lithospheric structure of the french massif central along 3 profiles to complete the maciv-bb broadband network to be deployed in 2024, france (resif-sismob).* RESIF - Réseau Sismologique et géodésique Français. Retrieved from https://seismology.resif.fr/networks/\#/XF__2024 doi: 10.15778/RESIF.XF2024

Paul Bedrosian, Jake R Morris, Margaret Goldman, & Benjamin R. Bloss. (2017). *Kansas and nebraska magnetotelluric time series (usgs-gggsc, kansas 2017 long period).* International Federation of Digital Seismograph Networks. Retrieved from https://www.fdsn.org/networks/detail/Z7_2017/ doi: 10.7914/SN/Z7_2017

Penn State University. (2004). *Pennsylvania state seismic network.* Interna-

tional Federation of Digital Seismograph Networks. Retrieved from https://www.fdsn.org/networks/detail/PE/ doi: 10.7914/SN/PE

Pieter-Ewald Share, & Frank Vernon. (2019). *Dense nodal deployment at some test sites for the upcoming faultscan project.* International Federation of Digital Seismograph Networks. Retrieved from https://www.fdsn.org/networks/detail/6E_2019/ doi: 10.7914/SN/6E_2019

Pilz, M., Ohrnberger, M., & Roux, P. (2023). *Meta-wt.* GFZ Data Services. Retrieved from https://geofon.gfz-potsdam.de/doi/network/XF/2023 doi: 10.14470/KS178126

Ramon Carbonell. (2012). *Wide-angle seismic reflection experiment across the central iberian zone; iberia peninsula.* International Federation of Digital Seismograph Networks. Retrieved from https://www.fdsn.org/networks/detail/7A_2012/ doi: 10.7914/SN/7A_2012

Regional Integrated Multi-Hazard Early Warning System (RIMES Thailand). (2008). *Regional integrated multi-hazard early warning system.* International Federation of Digital Seismograph Networks. Retrieved from https://www.fdsn.org/networks/detail/RM/ doi: 10.7914/SN/RM

Richards, F. D., Hoggard, M. J., Cowton, L. R., & White, N. J. (2018, October). Reassessing the Thermal Structure of Oceanic Lithosphere With Revised Global Inventories of Basement Depths and Heat Flow Measurements. *Journal of Geophysical Research: Solid Earth*, *123*(10), 9136–9161. Retrieved 2025-02-28, from https://agupubs.onlinelibrary.wiley.com/doi/10.1029/2018JB015998 doi: 10.1029/2018JB015998

Rick Aster, & Philip Kyle. (1999). *Mount erebus seismic studies.* International Federation of Digital Seismograph Networks. Retrieved from https://www.fdsn.org/networks/detail/XZ_1999/ doi: 10.7914/SN/XZ_1999

Ritter, J. R. R., Schmidt, B., Haberland, C., & Weber, M. (2014). *Deep-tee phase 1.* GFZ Data Services. Retrieved from https://geofon.gfz-potsdam.de/doi/network/1P/2014 doi: 10.14470/6C709520

Robert White. (2010). *Northern volcanic zone.* International Federation of Digital Seismograph Networks. Retrieved from https://www.fdsn.org/networks/detail/Z7_2010/ doi: 10.7914/SN/Z7_2010

Roger Hansen, & Gary Pavlis. (2005). *Collaborative research: St. elias erosion/tectonics project.* International Federation of Digital Seismograph Networks. Retrieved from https://www.fdsn.org/networks/detail/XZ_2005/ doi: 10.7914/SN/XZ_2005

Rufus Catchings. (2014). *2014 napa earthquake response.* International Federation of Digital Seismograph Networks. Retrieved from https://www.fdsn.org/networks/detail/7C_2014/ doi: 10.7914/SN/7C_2014

Ryberg, T., & Haberland, C. (2008). *Lake toba seismic network, sumatra, indonesia.* GFZ Data Services. Retrieved from http://geofon.gfz-potsdam.de/doi/network/7A/2008 doi: 10.14470/2N934755

S. De Angelis, & A. Diaz-Moreno. (2017). *Infra-etna.* International Federation of Digital Seismograph Networks. Retrieved from https://www.fdsn.org/networks/detail/XF_2017/ doi: 10.7914/SN/XF_2017

Sarah Mader, Tobias Neuffer, & Sebastian Busch. (2022). *Db miss.* International Federation of Digital Seismograph Networks. Retrieved from https://www.fdsn.org/networks/detail/1P_2022/ doi: 10.7914/SN/1P_2022

Scripps Institution of Oceanography. (1986). *Global seismograph network - iris/ida.* International Federation of Digital Seismograph Networks. Retrieved from https://www.fdsn.org/networks/detail/II/ doi: 10.7914/SN/II

Servicio Geológico Colombiano. (1993). *Red sismologica nacional de colombia.* International Federation of Digital Seismograph Networks. Retrieved from https://www.fdsn.org/networks/detail/CM/ doi: 10.7914/SN/CM

Servicio Sismológico Nacional, Instituto de Geofísica, Universidad Nacional

Autónoma de México, México. (2017). *Mx.* Servicio Sismológico Nacional, Instituto de Geofísica, Universidad Nacional Autónoma de México, México. Retrieved from http://www.ssn.unam.mx doi: 10.21766-ssnmx-sn-mx

Seton, M., Müller, R. D., Zahirovic, S., Williams, S., Wright, N. M., Cannon, J., ... McGirr, R. (2020, October). A Global Data Set of Present-Day Oceanic Crustal Age and Seafloor Spreading Parameters. *Geochemistry, Geophysics, Geosystems*, *21*(10). Retrieved 2025-07-21, from https://agupubs.onlinelibrary.wiley.com/doi/10.1029/2020GC009214 (Publisher: American Geophysical Union (AGU)) doi: 10.1029/2020gc009214

Silvio De Angelis. (2018). *Experiment in fuego.* International Federation of Digital Seismograph Networks. Retrieved from https://www.fdsn.org/networks/detail/XZ_2018/ doi: 10.7914/SN/XZ_2018

SOCQUET, A., BAEZ, J. C., MORENO, M., LANGLAIS, M., DEEP-Trigger Team, Geophysics Technical Service At ISTerre, & RESIF. (2020). *Deep_trigger temporary experiment in the subduction zone peru/chile, chile (resif-sismob).* RESIF - Réseau Sismologique et géodésique Français. Retrieved from https://seismology.resif.fr/fr/reseaux/\#/XZ__2020 doi: 10.15778/RESIF.XZ2020

Sridhar Anandakrishnan. (1995). *Antarctic microearthquake project, monitoring of ice stream c, west antarctica.* International Federation of Digital Seismograph Networks. Retrieved from https://www.fdsn.org/networks/detail/XF_1995/ doi: 10.7914/SN/XF_1995

Stein, C. A., & Stein, S. (1992). *A model for the global variation in oceanic depth and heat flow with lithospheric age.*

Steve Day, & Frank Vernon. (1994). *Peninsular range.* International Federation of Digital Seismograph Networks. Retrieved from https://www.fdsn.org/networks/detail/XF_1994/ doi: 10.7914/SN/XF_1994

Steve Grand, & Jim Ni. (2006). *Mapping the rivera subduction zone.* International Federation of Digital Seismograph Networks. Retrieved from https://www.fdsn.org/networks/detail/XF_2006/ doi: 10.7914/SN/XF_2006

Steve Grand, & Jim Ni. (2009). *Collaborative research: Northeast china extended seismic array: Deep subduction, mantle dynamics and lithospheric evolution beneath northeast china.* International Federation of Digital Seismograph Networks. Retrieved from https://www.fdsn.org/networks/detail/YP_2009/ doi: 10.7914/SN/YP_2009

Susan Bilek. (2024). *Bedload monitoring - flume test.* International Federation of Digital Seismograph Networks. Retrieved from https://www.fdsn.org/networks/detail/6E_2024/ doi: 10.7914/Y85B-6956

Sylvie Leroy. (2003). *Dhofar seismic experiment.* International Federation of Digital Seismograph Networks. Retrieved from https://www.fdsn.org/networks/detail/XZ_2003/ doi: 10.7914/SN/XZ_2003

Thrastarson, S., Van Herwaarden, D.-P., Noe, S., Josef Schiller, C., & Fichtner, A. (2024, June). REVEAL: A Global Full-Waveform Inversion Model. *Bulletin of the Seismological Society of America*, *114*(3), 1392–1406. Retrieved 2025-02-18, from https://pubs.geoscienceworld.org/bssa/article/114/3/1392/637892/REVEAL-A-Global-Full-Waveform-Inversion-Model doi: 10.1785/0120230273

Tiberi, C., Gautier, S., & RESIF. (2020). *Hazard in tanzanian rift : Hatari (resif-sismob).* RESIF - Réseau Sismologique et géodésique Français. Retrieved from https://seismology.resif.fr/networks/\#/XF__2018 doi: 10.15778/RESIF.XF2018

Tilmann, F., Heit, B., Moreno, M., & González-Vidal, D. (2021). *Anillo.* GFZ Data Services. Retrieved from https://geofon.gfz-potsdam.de/doi/network/Y6/2020 doi: 10.14470/L17575324477

Tulane University, Louisiana State University, & University Louisiana Lafayette.

(2019). *Induced seismicity in louisiana.* International Federation of Digital Seismograph Networks. Retrieved from https://www.fdsn.org/networks/detail/Z7_2019/ doi: 10.7914/SN/Z7_2019

Universidad de Chile. (2012). *Red sismologica nacional.* International Federation of Digital Seismograph Networks. Retrieved from https://www.fdsn.org/networks/detail/C1/ doi: 10.7914/SN/C1

University of Nevada, Reno. (1971). *Nevada seismic network.* International Federation of Digital Seismograph Networks. Retrieved from https://www.fdsn.org/networks/detail/NN/ doi: 10.7914/SN/NN

University of Oregon. (1990). *Pacific northwest seismic network - university of oregon.* International Federation of Digital Seismograph Networks. Retrieved from https://www.fdsn.org/networks/detail/UO/ doi: 10.7914/SN/UO

University of Puerto Rico. (1986). *Puerto rico seismic network & puerto rico strong motion program.* International Federation of Digital Seismograph Networks. Retrieved from https://www.fdsn.org/networks/detail/PR/ doi: 10.7914/SN/PR

University of Washington. (1963). *Pacific northwest seismic network - university of washington.* International Federation of Digital Seismograph Networks. Retrieved from https://www.fdsn.org/networks/detail/UW/ doi: 10.7914/SN/UW

USGS Alaska Anchorage. (2000). *Usgs northern mariana islands network.* International Federation of Digital Seismograph Networks. Retrieved from https://www.fdsn.org/networks/detail/MI/ doi: 10.7914/SN/MI

Utrecht University (UU Netherlands). (1983). *Nars.* International Federation of Digital Seismograph Networks. Retrieved from https://www.fdsn.org/networks/detail/NR/ doi: 10.7914/SN/NR

Various Institutions. (1965). *International miscellaneous stations.* International Federation of Digital Seismograph Networks. Retrieved from https://www.fdsn.org/networks/detail/IM/ doi: 10.7914/VEFQ-VH75

Vergne, J., Doubre, C., & Leroy, S. (2014). *Seismic network 7c:dora experiment (resif-sismob).* RESIF - Réseau Sismologique et géodésique Français. Retrieved from https://seismology.resif.fr/networks/\#/7C__2009 doi: 10.15778/RESIF.7C2009

Vergne, J., & RESIF. (2021). *Rittershoffen (bas-rhin, france) dense nodal seismic array temporary experiment (resif-sismob).* RESIF - Réseau Sismologique et géodésique Français. Retrieved from https://seismology.resif.fr/networks/\#/Z7__2018 doi: 10.15778/RESIF.Z72018

Weisen Shen. (2023). *Career: A comprehensive seismic investigation to the crust and uppermost mantle beneath the south pole, east antarctica.* International Federation of Digital Seismograph Networks. Retrieved from https://www.fdsn.org/networks/detail/Y6_2023/ doi: 10.7914/TVW3-C709

Wenyuan Fan, Yihe Huang, & S. Shawn Wei. (2018). *Lake-induced earthquakes in lake erie.* International Federation of Digital Seismograph Networks. Retrieved from https://www.fdsn.org/networks/detail/7D_2018/ doi: 10.7914/SN/7D_2018

Wes Thelen, & Paul Bodin. (2009). *Yakima landslide ramp.* International Federation of Digital Seismograph Networks. Retrieved from https://www.fdsn.org/networks/detail/7D_2009/ doi: 10.7914/SN/7D_2009

Yuan, X., Schurr, B., Haberland, C., Abdybachaev, U., & Sharshebaev, A. (2019). *Multi-scale imaging of the main pamir thrust faults within the framework of catena project – climatic and tectonic natural hazards in central asia.* GFZ Data Services. Retrieved from https://geofon.gfz-potsdam.de/doi/network/7A/2019 doi: 10.14470/2N7564774946

Zaroli, C. (2016, November). Global seismic tomography using Backus-Gilbert inversion. *Geophysical Journal International*, *207*(2), 876–888. Retrieved 2020-

08-04, from https://academic.oup.com/gji/article-lookup/doi/10.1093/gji/ggw315 doi: 10.1093/gji/ggw315

Zhao, L., Paul, A., Solarino, S., & RESIF. (2016). *Seismic network yp: Cifalps temporary experiment (china-italy-france alps seismic transect).* RESIF - Réseau Sismologique et géodésique Français. Retrieved from https://seismology.resif.fr/networks/\#/YP_2012 doi: 10.15778/RESIF.YP2012

Zhou, Y., Dahlen, F. A., & Nolet, G. (2004, July). Three-dimensional sensitivity kernels for surface wave observables. *Geophysical Journal International*, *158*(1), 142–168. Retrieved 2020-08-04, from https://academic.oup.com/gji/article-lookup/doi/10.1111/j.1365-246X.2004.02324.x doi: 10.1111/j.1365-246X.2004.02324.x

Zhou, Y., Nolet, G., Dahlen, F. A., & Laske, G. (2006). Global upper-mantle structure from finite-frequency surface-wave tomography. *Journal of Geophysical Research*, *111*(B04304). Retrieved 2020-08-04, from http://doi.wiley.com/10.1029/2005JB003677 doi: 10.1029/2005JB003677